RSC Advances

PAPER

View Article Online
View Journal | View Issue

Cite this: *RSC Adv.*, 2021, **11**, 15030

A DNA small molecular probe with increasing K^+ concentration promoted selectivity†

Ya-Ping Gong,[ab] Jian Yang,[c] Ji-Wang Fang,[ac] Qian Li,[b] Zhi-Yong Yu,*[a] Aijiao Guan *[b] and Han-Yuan Gong *[c]

Received 19th July 2020
Accepted 28th March 2021

DOI: 10.1039/d0ra06274j

rsc.li/rsc-advances

DNA small molecular probe study was considered as a promising approach to achieve DNA related disease diagnosis. Most related reports were performed under specific salinity. Herein, 4-imino-3-(pyridin-2-yl)-4*H*-quinolizine-1-carbonitrile (**IPQC**) was generated *via* a facile procedure with high yield (85%). It is found that **IPQC** could act as a universal probe for most tested ssDNA, dsDNA and G4 DNA in low $[K^+]$ concentration (less than 20 mM). However, **IPQC** showed highly selective G4 DNA binding *via* UV-vis and fluorescence response in increasing $[K^+]$ (*e.g.*, 150 mM) conditions. The ion atmosphere effects are instructive for DNA probe exploration. This provides guidance for the design, selection and optimization of the probes for target DNA sensing.

Introduction

Nucleic acid is the key genetic material in biological systems.[1–3] Its structural integrity determines physiological functions, cell proliferation, and/or differentiation.[4,5] DNA small molecular probes were developed to detect specific DNA species,[6–9] also their different folding types (*e.g.* G-quadruplex (G4), considered as a tumor marker species).[10–19] Up to now, probe study was considered as a promising approach to realize DNA related disease diagnosis.[20–26] However, most reported interactions between DNA and small molecular probes were explored under an environment with specific salinity.[27–32] Ion atmosphere effects were considered as a critical factor in DNA recognition. However, only limited examples involving the important effects were reported. These reports included the sodium concentration effect on the complexation between DNA and protein,[33] as well as the binding between ligand and double-stranded DNA (dsDNA).[34] Understanding and using ion atmosphere effects to promote specific DNA (such as G4) recognition is still under development.

Herein, we reported an unusual DNA small molecular probe, 4-imino-3-(pyridin-2-yl)-4*H*-quinolizine-1-carbonitrile (**IPQC**) with high K^+ concentration dependent selectivity. In low $[K^+]$ environment (*i.e.*, $[K^+] \leq 20$ mM), **IPQC** shows obvious UV-vis and/or fluorescence responses for most additional DNA species. The tested DNAs include ssDNA (*e.g.*, ssVEGF, ssPS1c-a, ssPS1c-b, ssAf17, ssG-tripl and ssT30), dsDNA (including dsPS1c, ds19AT, dsDx12, ds20, ds22, ds26 and 15GC), and G4 DNA (involving VEGF, bcl-2, H22, P21, c-myc and c-kit). Surprisingly, increasing $[K^+]$ improved the DNA recognition selectivity of **IPQC**. 150 mM $[K^+]$ (an intracellular K^+ concentration) induces **IPQC** response only for some additional G4 (Scheme 1). Such findings suggested that ion atmosphere effects (*e.g.*, $[K^+]$) in DNA detection should not be ignored in either exploring new or re-examining previous probes. The ion atmosphere effect study in the DNA detection will provide guidance for the design, selection and optimization of target DNA post-probes.

Experimental

Reagents and chemicals

All oligonucleotides were synthesized by Invitrogen (Beijing, China) and purified by ultra-polyacrylamide gel electrophoresis

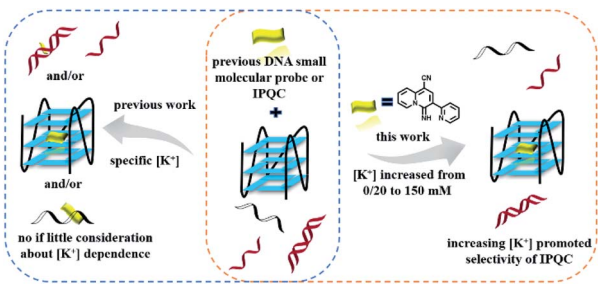

Scheme 1 The binding selectivity of previous DNA probe (left, in specific salinity (*i.e.*, $[K^+]$)) and **IPQC** probe (right) with increasing salinity (*e.g.*, $[K^+]$) promoted selectivity for G4 DNA sensing.

[a]*Department of Chemistry, Renmin University of China, Beijing, 100872, P. R. China*
[b]*Institute of Chemistry, Chinese Academy of Sciences, Zhongguancunbeiyijie 2, Beijing 100190, P. R. China*
[c]*College of Chemistry, Beijing Normal University, Xinjiekouwaidajie 19, Beijing 100875, P. R. China. E-mail: hanyuangong@bnu.edu.cn*

† Electronic supplementary information (ESI) available: UV-vis, fluorescence, NMR, HRMS and X-ray single crystal diffraction data. CCDC 1977107. For ESI and crystallographic data in CIF or other electronic format see DOI: 10.1039/d0ra06274j

(ULTRAPAGE) (purity 95%). Chemicals were purchased from Beijing Chem. Co. (China) and used without further purification. Ultrapure water was prepared by Milli-Q Gradient ultrapure water system (Millipore) and used throughout the experiments.

Sample preparation

The stock solutions of the oligonucleotides were prepared by dissolving oligonucleotides into the mixture containing ethanol and Tris–HCl buffer ([Tris] = 20 mM; the ratio between ethanol and aqueous phase as 1 : 99, v/v, pH = 7.2, containing 0, 20 or 150 mM KCl, respectively) and annealed in a thermocycler (first heating at 90 °C for 5 min, and slowly cooled down to room temperature, then stored at 4 °C before use). The concentration of oligonucleotides was determined based on their absorbance at 260 nm, dsDNA was prepared by heat denaturing and annealing the mixture of ssDNA1 and ssDNA2 (1 : 1). Stock solutions of **IPQC** were prepared in ethanol (2.00×10^{-3} M).

Synthesis of IPQC

2-Pyridylacetonitrile (1, 0.24 g, 2 mmol), sodium bis(trimethylsilyl)-amide (NaHMDS) (0.55 g, 3 mmol) and anhydrous DMF (5 mL) were added into an oven-dried 25 mL Schleck tube and then heated at 100 °C under air for 3 h. Cooling the mixture down to room temperature and then filtered. Collecting the liquid phase and removing solvent under reduced pressure, the residue was purified by column chromatography on silica gel (200–300 mesh, eluent as the mixture of acetone and petroleum ether (1/3, v/v) to afford the corresponding product as red-brown solid (0.42 g, 85% yield). Its structure was fully characterized *via* ^{1}H-NMR, ^{13}C-NMR, high resolution mass spectrometry (HRMS) and X-ray single crystal diffraction study.

Complexation study between IPQC and DNAs

The absorption spectra were recorded on an Agilent 8453 UV-visible spectrophotometer at the wavelength range 190–1100 nm using a 1 cm quartz cuvette. UV-vis absorbance titrations were carried out by preparing a series of mixture containing **IPQC** and DNAs. Concentration of **IPQC** kept as 2.00×10^{-5} M. Additional DNAs concentrations were changed from 0 to 4.0 molar equiv. of **IPQC**. The solution contained KCl as 0, 20 or 150 mM at room temperature in a special mixture solvent used in all the tests shown below (*i.e.*, ethanol–Tris–HCl buffer; which contained ethanol and Tris–HCl buffer ([Tris] = 20 mM; the ratio between ethanol and aqueous phase as 1 : 99, v/v, pH = 7.2)). The solvent mixture, each absorption spectrum was carried out after the sample incubation for 2 h.

Fluorescence spectra were recorded on a HITACHI F-4600 fluorescence spectrophotometer (Hitachi Limited, Japan). Fluorescence titration experiments were carried out with the same samples used in the UV-vis titration study. Fluorescence spectroscopic Job-plot was used to determine the binding stoichiometry. The total concentration of **IPQC** and DNAs were maintained as 2.00×10^{-5} M, with the molar ratio between **IPQC** and DNAs as 1 : 0, 5 : 1, 4 : 1, 3 : 1, 2 : 1, 1.5 : 1, 1 : 1, 1 : 1.5, 1 : 2, 1 : 3, 1 : 4 and 1 : 5, respectively.

CD (circular dichroism) spectra were collected on a Jasco 815 spectropolarimeter in a 2 mm path-length quartz cell. CD spectra of DNAs (2.00×10^{-5} M) were measured in the absence or presence of 1.0 molar equiv. of **IPQC**. ^{1}H-NMR and ^{13}C-NMR spectra were recorded on Bruker AVANCE 400. The single crystals used to obtain the X-ray diffraction structure grew clear light red cube. The .cif documents are available as separate ESI† files, which provide details regarding the specific crystal used for the analysis, along with the structure in question. Diffraction grade crystals were obtained *via* slow evaporation from solution using a mixture of dichloromethane/*n*-hexane.

Results and discussion

Although the synthetic method of **IPQC** was demonstrated in previous studies,[35] its properties are still under exploration. The previous synthetic route contained three steps with overall yield

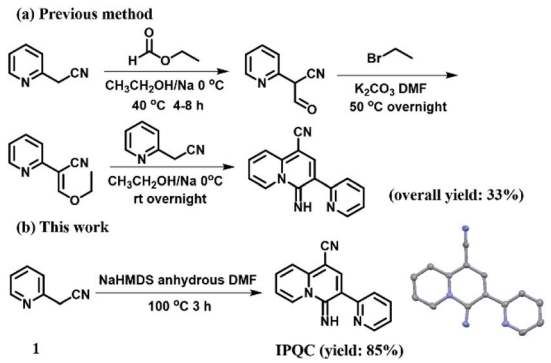

Fig. 1 The comparison between previous (a) and this (b) synthetic routes of IPQC.

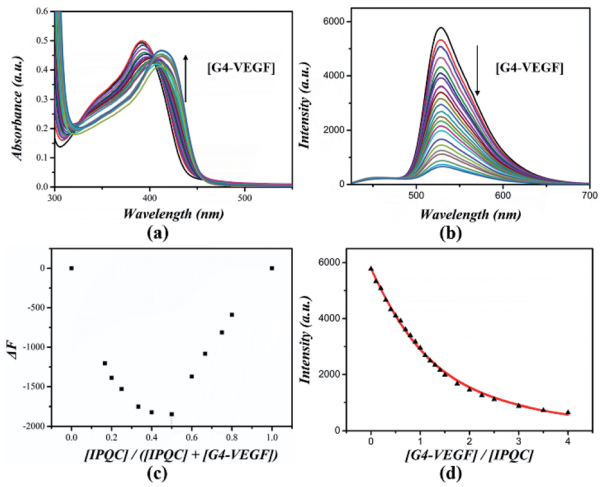

Fig. 2 The spectral changes of IPQC (2.00×10^{-5} M) in UV-vis (a) and fluorescence (b) with the increasing of G4-VEGF (from 0 to 4.0 molar equiv.); The Job-plot (c) and fluorescence titration (d) in ethanol–Tris–HCl buffer with [KCl] as 20 mM.

of 33%. Low yield, cumbersome steps and the use of hazardous reagents restrict its further exploration. Herein, the improved 'one-pot' reaction providing 'one pot' facile synthetic steps and high yield (85%). The efficient synthetic route will facilitate the subsequent property study (Fig. 1).

The UV-vis and fluorescence spectroscopic properties of **IPQC** were characterized. The related experiments were carried out in ethanol–Tris–HCl buffer. It is noted that 1% ethanol was added due to the limited solubility of **IPQC** in pure water phase. Finally, **IPQC** reveals a peak at $\lambda = 392$ nm with $\varepsilon_{392\ \mathrm{nm}} = 2.57 \times 10^4\ \mathrm{mol^{-1}\ L\ cm^{-1}}$ in UV-vis absorption. Fluorescence spectrum recorded at $\lambda_{ex} = 392$ nm showed a strong green emission peak of 528 nm, with fluorescence quantum yield $\Phi = 0.35$ and lifetime as 4.84 ns.

Cationic H^+·**IPQC** was believed as the form of **IPQC** in aqueous phase under pH around 7 (note: the pK_b value of **IPQC** is deduced as around 9.15 from the value of analogic quinoline). The pH dependent fluorescence spectra of 2.00×10^{-5} M **IPQC** show obvious change with pH value scale as 2 to 12 (*cf.* ESI Fig. S68 and S69†). It suggests that H^+·**IPQC** is the main form with pH around 7. The planar skeleton and protonation induce the expectation to use **IPQC** as a potential biological probe of anionic biological macromolecules (*e.g.*, nucleic acids), as the well-known G-quartet ligand, berberine.[36–38]

As initial work, we investigated the interaction between **IPQC** and a series of DNA structures (*cf.*, Table S1†). G-quadruplex VEGF (Vascular Endothelial Growth Factor, a cancer treatment target)[39–41] was selected for the first test. UV-vis absorption peak of **IPQC** at $\lambda = 392$ nm red-shifts 19 nm with adding 4.0 molar equiv. of G4-VEGF. Meanwhile, obvious intensity decreasing was shown in fluorescence emission spectrum (carried out in ethanol–Tris–HCl buffer with [KCl] as 20 mM). The decreasing

Table 1 K_a (M^{-1}) calculated *via* UV-vis or fluorescence titration[a]

		K_a measurement in $[K^+]$ as 0 or 20 mM		K_a measurement in $[K^+]$ as 150 mM	
		Method		Method	
Substrate (S)	[**IPQC**] : [S]	UV-vis	Fluorescence	UV-vis	Fluorescence
G4-bcl-2	1 : 1	$(5.0 \pm 0.2) \times 10^5$	$(2.5 \pm 0.1) \times 10^5$	$(1.6 \pm 0.1) \times 10^5$	$(2.5 \pm 0.1) \times 10^5$
	1 : 2	$(7.9 \pm 0.4) \times 10^4$	$(1.3 \pm 0.1) \times 10^5$	$(5.0 \pm 0.3) \times 10^4$	$(2.5 \pm 0.1) \times 10^4$
	2 : 3	$(3.2 \pm 0.3) \times 10^4$	$(2.0 \pm 0.2) \times 10^3$	$(1.3 \pm 0.1) \times 10^4$	$(4.0 \pm 0.3) \times 10^3$
G4-H22	1 : 1	$(7.9 \pm 0.2) \times 10^4$	$(1.0 \pm 0.1) \times 10^5$	$(2.0 \pm 0.1) \times 10^4$	$(1.3 \pm 0.1) \times 10^4$
	1 : 2	$(6.3 \pm 0.3) \times 10^4$	$(2.5 \pm 0.1) \times 10^4$	—	—
	2 : 3	$(2.0 \pm 0.2) \times 10^5$	$(7.9 \pm 0.6) \times 10^4$	—	—
G4-P21	1 : 1	$(7.9 \pm 0.2) \times 10^4$	$(7.9 \pm 0.2) \times 10^4$	$(1.3 \pm 0.1) \times 10^4$	$(1.0 \pm 0.1) \times 10^4$
	1 : 2	$(1.3 \pm 0.1) \times 10^5$	$(1.3 \pm 0.1) \times 10^5$	—	—
	2 : 3	$(2.5 \pm 0.2) \times 10^4$	$(2.5 \pm 0.2) \times 10^4$	—	—
G4-VEGF	1 : 1	$(1.3 \pm 0.1) \times 10^5$	$(7.9 \pm 0.2) \times 10^4$	$(2.5 \pm 0.1) \times 10^4$	$(2.0 \pm 0.1) \times 10^4$
G4-c-kit	1 : 1	$(5.0 \pm 0.2) \times 10^5$	$(3.2 \pm 0.1) \times 10^5$	$(2.0 \pm 0.1) \times 10^5$	$(1.3 \pm 0.1) \times 10^5$
	1 : 2	$(1.0 \pm 0.1) \times 10^4$	$(7.9 \pm 0.4) \times 10^3$	$(1.6 \pm 0.1) \times 10^4$	$(1.6 \pm 0.1) \times 10^4$
	2 : 3	$(2.5 \pm 0.2) \times 10^3$	$(5.0 \pm 0.4) \times 10^3$	$(4.0 \pm 0.3) \times 10^4$	$(4.0 \pm 0.3) \times 10^3$
G4-c-myc	1 : 1	$(6.3 \pm 0.2) \times 10^5$	$(7.9 \pm 0.2) \times 10^5$	$(1.6 \pm 0.1) \times 10^5$	$(5.0 \pm 0.2) \times 10^4$
	1 : 2	$(1.0 \pm 0.1) \times 10^5$	$(3.2 \pm 0.2) \times 10^4$	$(6.3 \pm 0.3) \times 10^4$	$(7.9 \pm 0.4) \times 10^4$
	2 : 3	$(5.0 \pm 0.4) \times 10^4$	$(2.0 \pm 0.2) \times 10^5$	$(1.0 \pm 0.1) \times 10^5$	$(5.0 \pm 0.4) \times 10^4$
ds20	1 : 1	$(1.6 \pm 0.1) \times 10^4$	$(2.0 \pm 0.1) \times 10^4$	—	—
ds22	1 : 1	$(2.0 \pm 0.1) \times 10^5$	$(2.0 \pm 0.1) \times 10^5$	—	—
	1 : 2	$(1.6 \pm 0.1) \times 10^4$	$(1.3 \pm 0.1) \times 10^4$		
	2 : 3	$(1.3 \pm 0.1) \times 10^6$	$(3.2 \pm 0.3) \times 10^5$		
ds26	1 : 1	$(5.0 \pm 0.2) \times 10^4$	$(8.0 \pm 0.2) \times 10^4$	—	—
	1 : 2	$(1.0 \pm 0.1) \times 10^4$	$(6.3 \pm 0.3) \times 10^3$		
	2 : 3	$(7.9 \pm 0.6) \times 10^4$	$(1.6 \pm 0.1) \times 10^4$		
ds19AT	1 : 1	$(3.2 \pm 0.1) \times 10^4$	$(3.2 \pm 0.1) \times 10^4$	—	—
dsDx12	1 : 1	$(7.9 \pm 0.2) \times 10^4$	$(6.3 \pm 0.2) \times 10^4$	—	—
hairpin15GC	1 : 1	—	$(5.0 \pm 0.2) \times 10^4$	—	—
ssVEGF	1 : 1	$(5.0 \pm 0.2) \times 10^4$	$(6.3 \pm 0.2) \times 10^4$	—	—
ssPS1c-a	1 : 1	—	—	—	—
ssAf17	1 : 1	—	—	—	—
ssG-tripl	1 : 1	—	—	—	—
dsPS1c	—	—	—	—	—
ssPS1c-b	—	—	—	—	—
ssT30	—	—	—	—	—

[a] (1) Equations governing the relevant equilibria: $[H] + [G] \overset{K_{a1}}{\rightleftharpoons} [HG][HG] + [G] \overset{K_{a2}}{\rightleftharpoons} [HG_2][HG] + [HG_2] \overset{K_{a3}}{\rightleftharpoons} [H_2G_3]$, here H indicated **IPQC** and G for various DNA substrates. (2) '—' indicates titration experiments are unsuccessful because of the weak response of **IPQC** to additional DNAs. (3) All the tests were carried out in buffer ([Tris] = 20 mM; the ratio between ethanol and aqueous phase as 1 : 99, v/v, pH = 7.2). 20 or 150 mM KCl was used in G4 DNA tests, 0 or 150 mM KCl was used in the cases of ss/ds DNAs.

fluorescence intensity attributed mainly to the $H^+ \cdot$**IPQC** binding on the surface of G4-VEGF *via* π–π stacking interaction *via* molecular simulation (*cf.* Fig. 4a–c). Other synergistic effects, such as electrostatic attraction between negative DNA and positive $H^+ \cdot$**IPQC**, suitable shape and volume of $H^+ \cdot$**IPQC** to the groove, also may lead to the fluorescence quenching of $H^+ \cdot$**IPQC**.

Further CD (circular dichroism) experiments showed DNA signals are almost the same before and after adding **IPQC**, while **IPQC** has no Cotton effect in the presence or absence of DNA species (*cf.* ESI Fig. S73†). This phenomenon indicates DNA configuration is kept during the binding process. The stoichiometric ratio between **IPQC** and DNA were speculated by Job-plot analysis, despite the method is limited in some complicated cases.[42–44] Fluorescence Job-plot analysis resulted in a minimum value at [**IPQC**]/([**IPQC**] + [G4-VEGF]) ratio as 0.5. The finding suggested a 1 : 1 binding stoichiometry (Fig. 2). Further UV-vis titration experiment suggested the association constant $K_{a1} = (1.3 \pm 0.1) \times 10^5\ M^{-1}$ for the 1 : 1 complexation. The result is consistent with calculated $K_{a1} = (7.9 \pm 0.2) \times 10^4\ M^{-1}$ from fluorescence titration.

Same methods were also used to study the interactions between **IPQC** and other tested DNAs. The association constants were summarized in Table 1 and Fig. 3, which exhibit both obvious UV-vis and fluorescence signal response in most cases involving ssDNA, dsDNA, and G-quadruples.

For further *in vivo* and/or *in situ* detection, we studied the DNA sensing behaviour of **IPQC** in simulated physiological environment. Specifically, the interaction between **IPQC** and former tested DNAs were explored in ethanol–Tris–HCl buffer with 150 mM K^+ (an intracellular K^+ concentration). Surprisingly, **IPQC** exhibits both UV-vis and fluorescence response only for G-quadruplex in this condition, while the responses for all the tested ss/ds DNA disappeared. Specifically, the association constant value $K_{a1} = (2.0 \pm 0.1) \times 10^4\ M^{-1}$ between **IPQC** and G4-VEGF indicates that excess potassium do not strongly weaken combination between **IPQC** and G4-VEGF. As Fig. 3 shows, although the affinity between other G-quadruplex and probe **IPQC** may be slightly weakened with increasing [K^+], they all show similar spectral response. The K_{a1} value of the 1 : 1 binding calculated by UV-vis and fluorescence titration has no significant change compared with which in low [K^+] system.

20 mM magnesium ions and 10 mM sodium ions were added to ethanol–Tris–HCl buffer with 150 mM K^+ to further mimic the intracellular environment (*cf.* ESI Fig. S74–S79†). The final spectral responses (especially in fluorescence spectrum) are observed as the same as before adding. It implied that the high selectivity of **IPQC** for G4 remains after adding 20 mM $MgCl_2$ and 10 mM NaCl. The result proves high [K^+] (150 mM) promoted high selectivity of **IPQC** for G-quadruplex binding.

To further explore the increasing selectivity of **IPQC**, K^+ concentrate dependent effect between **IPQC** and dsDNA was studied in detail *via* UV-vis and fluorescence methods. Additional dsDNA induced spectral response of **IPQC** was carried out. The spectroscopic changes decline with adding [K^+], until completely disappear with [K^+] as 500 mM (*cf.* Fig. S82–S84†). This experiment interpreted that intermolecular interactions between dsDNA and probe **IPQC** are acutely sensitive to ion atmosphere effects. To deeper insight of the phenomena, molecular modelling was carried out. It revealed that **IPQC** can stack on the surface of the terminal quartet of G4 DNA (Fig. 4) or insert into the groove of ss/dsDNA structure in low [K^+]. It is suggested that excess cations can compete with protonated **IPQC** to bind DNA (*cf.* ESI Fig. S70 and S71†). Furthermore, K^+ bind with polyanionic DNA helix to reduce electrostatic repulsion of the negative charges on DNA phosphate backbone. It is unfavourable for **IPQC** to intercalate to the groove binding sites in ss/dsDNAs. As the result, the binding between **IPQC** and ss/dsDNA weakens or even disappears with increasing K^+. Differently, in the cases of G4 DNAs, the presence of metal cation (*e.g.*, Li^+, Na^+ or K^+) benefit to form a metal-ion-stabilized G4

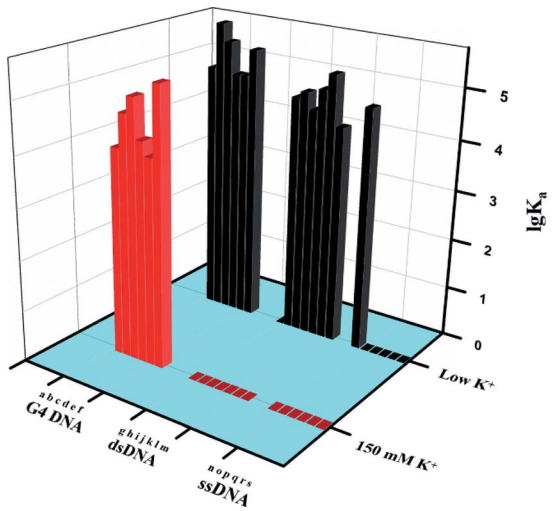

Fig. 3 Lg K_a histogram of **IPQC** and DNAs (a: H22, b: c-myc, c: c-kit; d: VEGF; e: P21; f: bcl-2; g: dsPs1c; h: hairpin15GC; i: dsDx12; j: ds19AT; k: ds26; l: ds22; m: ds20; n: ssVEGF; o: ssPs1c-a; p: ssPs1c-b; q: ssAf17; r: ssG-tripl; s:ssT30) calculated from fluorescence titration in ethanol–Tris–HCl buffer with low (0 or 20 mM) or 150 mM KCl.

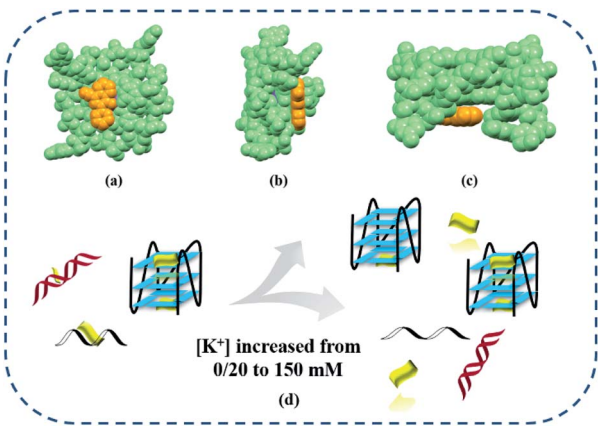

Fig. 4 The top (a), side (b) and front (c) views of the optimal structure of 1 : 1 complexation between G4 VEGF (light green) and **IPQC** (orange) are shown as molecular surface; the binding changes between DNAs and **IPQC** with [K^+] varying from 0/20 to 150 mM.

structures (although Li^+ provide inefficient induction for G4 structure formation[45–47]) so that the electron-rich quinoline plane of **IPQC** can effectively sit on the planar surface of the G-quadruplex *via* π–π stacking (*cf.* ESI Fig. S80 and S81†). Finally, the electrostatic completion of K^+ and the enhancement of ion atmosphere effect shown above led a net result as little influence on the binding process between G4 and **IPQC** sitting on the G-quadruplex. However, the other G4 binding mode(s) of **IPQC** will also be weaken as the cases of ss/ds DNAs. Actually, the binding stoichiometries between **IPQC** and some G4 DNAs (*e.g.*, G4-H22 or G4-P21) change from 2 : 3 to 1 : 1 corresponding to $[K^+]$ as 20 or 150 mM, respectively (*cf.* ESI Fig. S67†).

Conclusions

In conclusion, molecule 4-imino-3-(pyridin-2-yl)-4*H*-quinolizine-1-carbonitrile (**IPQC**) was efficiently synthesized *via* a simple one-pot method. It exhibits high selectivity to G-quadruplex compared to ss/dsDNA in sufficient $[K^+]$, it even acts as a universal DNA probe for ss/ds and G4 DNA under low $[K^+]$ (0 or 20 mM) environment. Ion atmosphere effects induced selectivity urges us to re-examine the previous DNA probes and provide more perspective for the design of new ones.

Conflicts of interest

There are no conflicts to declare.

Acknowledgements

This research was supported under the National Natural Science Foundation of China (Grant numbers 21303225, 21675162, 21977096, 21778058, 21672025, 21472014, 21971022), the Beijing Natural Science Foundation (Grant Number 7182189 and 7172248).

Notes and references

1 I. Ahmad, A. Ahmad and M. Ahmad, *Phys. Chem. Chem. Phys.*, 2016, **18**, 6476–6485.
2 A. Mukherjee, S. Mondal and B. Singh, *Int. J. Biol. Macromol.*, 2017, **101**, 527–535.
3 K. Gracie, V. Dhamodharan, P. I. Pradeepkumar, K. Faulds and D. Graham, *Analyst*, 2014, **139**, 4458–4465.
4 A. Subastri, C. H. Ramamurthy, A. Suyavaran, R. Mareeswaran, P. Lokeswara Rao, M. Harikrishna, M. Suresh Kumar, V. Sujatha and C. Thirunavukkarasu, *Int. J. Biol. Macromol.*, 2015, **78**, 122–129.
5 F. Wu, J. Jin, L. Wang, P. Sun, H. Yuan, Z. Yang, G. Chen, Q.-H. Fan and D. Liu, *ACS Appl. Mater. Interfaces*, 2015, **7**, 7351–7356.
6 M. Jin, X. Liu, X. Zhang, L. Wang, T. Bing, N. Zhang, Y. Zhang and D. Shangguan, *ACS Appl. Mater. Interfaces*, 2018, **10**, 25166–25173.
7 S. N. Journey, S. L. Alden, W. M. Hewitt, M. L. Peach, M. C. Nicklaus and J. S. Schneekloth Jr, *Med. Chem. Comm.*, 2018, **9**, 2000–2007.
8 W. Gai, Q. Yang, J. Xiang, W. Jiang, Q. Li, H. Sun, A. Guan, Q. Shang, H. Zhang and Y. Tang, *Nucleic Acids Res.*, 2013, **41**, 2709–2722.
9 L. Yu, Q. Yang, J. Xiang, H. Sun, L. Wang, Q. Li, A. Guan and Y. Tang, *Analyst*, 2015, **140**, 1637–1646.
10 M.-H. Hu, S.-B. Chen, R.-J. Guo, T.-M. Ou, Z.-S. Huang and J.-H. Tan, *Analyst*, 2015, **140**, 4616–4625.
11 A. C. Bhasikuttan and J. Mohanty, *Chem. Commun.*, 2015, **51**, 7581–7597.
12 A. C. Bhasikuttan, J. Mohanty and H. Pal, *Angew. Chem., Int. Ed.*, 2007, **46**, 9305–9307.
13 H. Chen, H. Sun, S. Zhang, W. Yan, Q. Li, A. Guan, J. Xiang, M. Liu and Y. Tang, *Chem. Commun.*, 2019, **55**, 5060–5063.
14 M. Liu, Y. Liu, F. Wu, Y. Du and X. Zhou, *Bioorg. Med. Chem.*, 2019, **27**, 1962–1965.
15 T. M. Ou, Y. J. Lu, J. H. Tan, Z. S. Huang, K. Y. Wong and L. Q. Gu, *ChemMedChem*, 2008, **3**, 690–713.
16 L. L. Tong, L. Li, Z. Chen, Q. Wang and B. Tang, *Biosens. Bioelectron.*, 2013, **49**, 420–425.
17 S. Zhang, H. Sun, L. Wang, Y. Liu, H. Chen, Q. Li, A. Guan, M. Liu and Y. Tang, *Nucleic Acids Res.*, 2018, **46**, 7522–7532.
18 D. Wei, A. K. Todd, M. Zloh, M. Gunaratnam, G. N. Parkinson and S. Neidle, *J. Am. Chem. Soc.*, 2013, **135**, 19319–19329.
19 G. N. Parkinson and G. W. Collie, *G-Quadruplex Nucleic Acids*, 2019, 131–155.
20 L. Zhou, J. Yang, C. Estavillo, J. D. Stuart, J. B. Schenkman and J. F. Rusling, *J. Am. Chem. Soc.*, 2003, **125**, 1431–1436.
21 D. Gibson, *Pharmacogenomics J.*, 2002, **2**, 275–276.
22 L. Xie, X. Qian, J. Cui, Y. Xiao, K. Wang, P. Wu and L. Cong, *Bioorg. Med. Chem.*, 2008, **16**, 8713–8718.
23 A. J. Pickard, F. Liu, T. F. Bartenstein, L. G. Haines, K. E. Levine, G. L. Kucera and U. Bierbach, *Chem. –Eur. J.*, 2014, **20**, 16174–16187.
24 A. Rajendran and B. U. Nair, *Biochim. Biophys. Acta*, 2006, **1760**, 1794–1801.
25 M. Gunaratnam, G. W. Collie, A. P. Reszka, A. K. Todd, G. N. Parkinson and S. Neidle, *Bioorg. Med. Chem.*, 2018, **26**, 2958–2964.
26 M. Sayed and H. Pal, *Phys. Chem. Chem. Phys.*, 2015, **17**, 9519–9532.
27 C. C. Chang, J. Y. Wu, C. W. Chien, W. S. Wu, H. Liu, C. C. Kang, L. J. Yu and T. C. Chang, *Anal. Chem.*, 2003, **75**, 6177–6183.
28 B. Jin, X. Zhang, W. Zheng, X. Liu, J. Zhou, N. Zhang, F. Wang and D. Shangguan, *Anal. Chem.*, 2014, **86**, 7063–7070.
29 M. Nikan, M. D. Antonio, K. Abecassis, K. McLuckie and S. Balasubramanian, *Angew. Chem., Int. Ed.*, 2013, **52**, 1428–1431.
30 D. Verga, C. H. N'Guyen, M. Dakir, J. L. Coll, M. P. Teulade-Fichou and A. Molla, *J. Med. Chem.*, 2018, **61**, 10502–10518.
31 M.-Q. Wang, Y. Zhang, X.-Y. Zeng, H. Yang, C. Yang, R.-Y. Fu and H.-J. Li, *Dyes Pigm.*, 2019, **168**, 334–340.
32 X.-f. Zhang, J.-f. Xiang, M.-y. Tian, Q.-f. Yang, H.-x. Sun, S. Yang and Y.-l. Tang, *J. Phys. Chem. B*, 2009, **113**, 7662–7667.

33 B. E. Allred, M. Gebala and D. Herschlag, *J. Am. Chem. Soc.*, 2017, **139**, 7540–7548.
34 M. T. Record Jr, T. M. Lohman and P. J. De Haseth, *J. Mol. Biol.*, 1976, **107**, 145–158.
35 Y.-F. Luo, T. Yang and Y.-Q. Wei, CN 107739375A, G01N21/64, 2018.
36 F. Papi, C. Bazzicalupi, M. Ferraroni, G. Ciolli, P. Lombardi, A. Y. Khan, G. S. Kumar and P. Gratteri, *ACS Med. Chem. Lett.*, 2020, **11**, 645–650.
37 Y. Ma, T. M. Ou, J. H. Tan, J. Q. Hou, S. L. Huang, L. Q. Gu and Z. S. Huang, *Eur. J. Med. Chem.*, 2011, **46**, 1906–1913.
38 I. Bessi, C. Bazzicalupi, C. Richter, H. R. Jonker, K. Saxena, C. Sissi, M. Chioccioli, S. Bianco, A. R. Bilia, H. Schwalbe and P. Gratteri, *ACS Chem. Biol.*, 2012, **7**, 1109–1119.
39 G. Martiny-Baron and D. Marmé, *Pharm. Technol.*, 1995, **6**, 675–680.
40 A. Bikfalvi and R. Bicknell, *Trends Pharmacol. Sci.*, 2002, **23**, 576–582.
41 D. Sun, K. Guo, J. J. Rusche and L. H. Hurley, *Nucleic Acids Res.*, 2005, **33**, 6070–6080.
42 F. Ulatowski, K. Dabrowa, T. Balakier and J. Jurczak, *J. Org. Chem.*, 2016, **81**, 1746–1756.
43 D. Brynn Hibbert and P. Thordarson, *Chem. Commun.*, 2016, **52**, 12792–12805.
44 J. S. Renny, L. L. Tomasevich, E. H. Tallmadge and D. B. Collum, *Angew. Chem., Int. Ed.*, 2013, **52**, 11998–12013.
45 T. J. Pinnavaia, C. L. Marshall, C. M. Mettler, C. L. Fisk, H. T. Miles and E. D. Becker, *J. Am. Chem. Soc.*, 1978, **100**, 3625–3627.
46 C. Bardin and J. L. Leroy, *Nucleic Acids Res.*, 2008, **36**, 477–488.
47 J. W. Shim, Q. Tan and L.-Q. Gu, *Nucleic Acids Res.*, 2009, **37**, 972–982.